4th USA/Europe Air Traffic Management R&D Seminar Santa Fe, 3-7 December 2001

Accident Risk Assessment of Simultaneous Converging Instrument Approaches

Henk A.P. Blom, Margriet B. Klompstra and Bert Bakker

National Aerospace Laboratory NLR, PO Box 90502, 1006 BM Amsterdam, The Netherlands
e-mails: blom@nlr.nl; klompstr@nlr.nl; bakker@nlr.nl

ABSTRACT

With increasing traffic there often are environmental and economical reasons to optimise Simultaneous Converging Instrument Approaches (SCIA) without sacrificing the high safety levels realised in air traffic. One of the well known safety issues of SCIA is the risk of a mid air collision due to a double go around. The aim of this paper is to show through a working example that there is a clear advantage to accomplish the safety protection through support of advanced accident risk assessment methodology. In this paper such methodology is applied to a specific example of SCIA at Schiphol airport. Comparison of the obtained results against FAA established SCIA criteria shows that there are situations in which these FAA criteria are not met, while the collision risk is not higher than for other situations that satisfy these criteria. The implication for Schiphol airport is that a specific change can be introduced as being risk neutral. The implication for other busy airports with converging runways might be that there is room to develop new or improved SCIA without compromising safety.

1. INTRODUCTION

Many airports in the world have converging runways. Due to increasing traffic, these airports have environmental and economical incentives to allow for Simultaneous Converging Instrument Approaches (SCIA) without compromising established safety levels. And if safe SCIA would not be feasible, then the next best option could be to allow for Dependent Converging Instrument Approaches (DCIA). One of the well known safety issues of SCIA/DCIA is to safely manage a double go around (GA). The basic studies on these safety management issues have been performed by MITRE; first for SCIA (Newman et al., 1981; Weiss, 1986), and later for DCIA (Smith et al., 1992). The analysis used in these basic studies consists of a systematic "worst" case reasoning about missed approaches, i.e. GA's that are not rejected landings. This might lead to safety conservative requirements on SCIA/DCIA. The aim of the current paper is to show through an example that the existing criteria of allowing SCIA indeed may be relaxed by systematically exploiting an accident risk assessment modelling approach(*).

(*) *Parts of this research have been performed with support of CAA and ATC The Netherlands.*

1.1 Existing SCIA criteria

Although ICAO provides criteria for simultaneous instrument operations on parallel or near parallel runways (ICAO, 1988), these criteria do not address SCIA. The FAA, however, has systematically developed SCIA criteria (FAA, 1993), which are often referred to as the TERPS+3 criteria, and which come down to:

1) Non-intersecting straight-in final approach courses;
2) Missed Approach Points (MAPt's), for latest yes/no landing decision, must be at least 3 nautical miles apart;
3) Published missed approach paths diverge by at least 45 degrees and the associated primary TERPS obstacle clearance surfaces (ICAO, 1996) do not overlap;
4) ATC shall designate separation responsibility and procedures to be applied in the event of a Rejected Landing, i.e. a GA initiated beyond the MAPt;
5) ATC may establish higher weather minima than published to preclude, to the extent feasible, the possibility of a weather related missed approach.

In McCartor et al. (1997), it has also been shown that properly equipped FMS aircraft that execute a missed approach on the autopilot could do much better than criterion 3) requires. In line with this, for a limited category of aircraft, criterion 3) has been tightened and criterion 2) has been replaced by the requirement that the MAPt on the secondary runway should not be lower than 650 feet (FAA, 1998).

For airports that frequently experience low ceiling conditions, the FAA criteria imply a serious limitation in the effective exploitation of SCIA, and a similarly frequent limitation of airport capacity. Hence from an airport capacity point of view it would be very valuable to have an approach that allows to relax the existing SCIA criteria.

1.2 Example considered

The particular example considered in this paper is SCIA on runways 19R and 22 of Schiphol airport, the geometry of which is depicted in Figure 1.

Runway 19R is one of Schiphol's four main runways. It has its MAPt at the threshold and has a straight missed approach path, while runway 22 is a secondary non-intersecting runway with its MAPt at 1 nautical mile before the threshold (height at ILS is about 350 feet) and a missed approach path that is 60 degrees turning left (AIP, 2000). Allowance of SCIA on

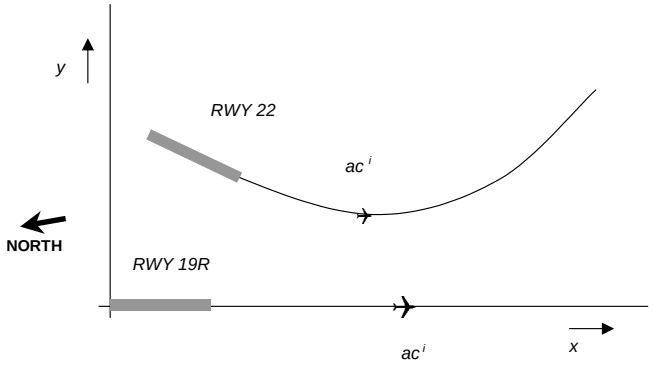

Figure 1 Geometry of runways 19R and 22 at Schiphol airport and the nominally performed missed approach paths.

runways 19R and 22 is limited to conditions of relatively high headwind for runway 22, and the two runway controllers are trained to safely manage double missed approaches even when the aircraft on 22 makes a straight missed approach. All together it can be verified that the TERPS+3 criteria of (FAA, 1993) are satisfied.

Frequent low ceiling conditions at Schiphol airport ask for a MAPt that is as close as possible to the threshold of runway 22. Unfortunately, such lowering of the MAPt-threshold distance would mean that TERPS+3 criterion number 2) is no longer satisfied for SCIA on runways 22 and 19R. In order to learn understanding this, a risk assessment modelling study has been conducted following the approach of (Blom et al., 1998). This modelling study has been organised in two phases:

- Phase 1, to develop an initial risk assessment model that is able to make a relative comparison of accident risks due to double GA's with the old and the new MAPt's.
- Phase 2, to further refine the risk assessment model to allow a comparison of the risk due to double GA's with established accident risk criteria for en-route traffic.

1.3 Phase 1 study

During phase 1, relative accident risk assessments have been performed for two situations: one with the MAPt for runway 22 at 1 Nm before the threshold, and the other with the MAPt shifted towards the threshold. The steps performed are:

- Identification of existing and new operations, including the relevant scenarios and the associated hazards, both through brainstorms and interviews with experts and through making use of dedicated hazard and incident data bases. The initial background material for this is collected in (Speijker et al., 2000).
- Development of the mathematical model, including model assumptions and assessment of parameter values, and integration with the identified scenarios. The background for this and the initial accident risk assessment is provided in (Blom et al., 2001a)

The key finding of phase 1 was that the developed model of the SCIA operation on 19R and 22 is risk neutral with respect to the proposed shifting of the MAPt for runway 22 towards its threshold. The rationale for this finding is that in the model the largest contribution to accident risk stems from a non-negligible probability that both aircraft follow a straight missed approach path.

1.4 Phase 2 study

The aim of the phase 2 study is to refine the risk assessment model and subsequently compare the double GA's risk of conducting SCIA on runways 19R×22 against established collision risk criteria. The steps performed are:

- In order to allow for a significant reduction of the level of uncertainty in the assessed risk, site-specific statistical data on go arounds and their reasons has been collected in collaboration with ATC The Netherlands.
- On the basis of this information, the accident risk assessment model and its assumptions have been further improved, and subsequently the modelled accident risk has been evaluated.
- Subsequently, a bias and uncertainty analysis has been performed following a recently developed approach (Everdij and Blom, 2001).
- Finally the obtained accident risk results have been compared against related risk criteria (ICAO, 1998) for collision between en-route flying aircraft.

1.5 Aim and organisation of this paper

This paper aims to present the phase 2 results and is organised as follows. Section 2 provides an overview of the main probabilistic models collected during both phases for the Schiphol example considered. Section 3 explains how these probabilistic models are integrated into a mathematical collision risk model. Section 4 introduces the specific Schiphol example scenarios that have been evaluated during phase 2, and gives the accident risk results obtained for these scenarios. Section 5 summarises the findings and draws conclusions regarding the specific Schiphol example and subsequently regarding the TERPS+3 criteria for SCIA in general.

2. MODELLING OF GO AROUNDS

One of the important steps required for accident risk assessment is to develop probabilistic models of go arounds. The aim of this section is to explain the main issues covered by this modelling:

- Landing traffic flows
- Go around frequencies
- Go around initiation height
- Go around climb behaviour
- Turn during go around
- Controller turn instruction

In addition to this, other probabilistic models have been adopted for issues such as aircraft speed behaviour, wind conditions and aircraft sizes. Details are given in (Blom et al., 2001c).

2.1 Landing traffic flows

Based on the evaluation of statistical data for the percentages of landing heavy/medium/light aircraft on runways 19R and 22, the following percentages of weight category arrival have been chosen for 19R and 22. This is referred to as **Model assumption M.1**. The arrival spread over the weight classes is based on radar data reconstructed arrival trajectories over several one month periods. This has shown that the uncertainty of assumption **M.1** is small.

	Arrivals on 19R	Arrivals on 22
Heavy	22%	0%
Medium	78%	85%
Light	0%	15%

Table 1 Arrival category percentages.

The traffic flow is assumed to be 30 arrivals per hour for each runway. This is referred to as **Model assumption M.37**. Furthermore it is assumed that none of this traffic is equipped with TCAS, and that no use is made of see-and-avoid. This is covered by **Model assumptions M.15** and **M.16** respectively.

2.2 Go around frequencies

During the first phase of the study there appeared to be significant uncertainty regarding the frequencies of go arounds (Blom et al., 2001a). During the second phase of the study this problem has been addressed through making use of the fact that since June 1995 tower controllers at Schiphol have systematically been reporting go arounds as part of the safety management process of ATC The Netherlands. This data set has been analysed in a statistical sense. The first analysis was directed towards the variety in reasons and the percentages, the result of which is depicted in Table 2 for both uncommon and potentially common causes.

Reason	Percentage
UNCOMMON CAUSES	**59.8 %**
Crew related	**4.2 %**
Misunderstood R/T	0.7 %
Wrong R/T frequency	1.3 %
Wrong approach charts	0.3 %
Cabin not ready	1.5 %
Unintended MA	0.5 %
Technical aircraft	**25.5 %**
Bird strike	0.9 %
Technical unknown	2.2 %
Technical various	1.1 %
Gear (door) problems	14.2 %
Flap problems	5.8 %
Autopilot / nav receiver	1.2 %
Unstable approach/landing	**24.9 %**
ILS failed	0.4 %
Wake turbulence	1.1 %
Unstable approach	5.7 %
Speed high	1.7 %
Altitude high	13.5 %
Ground Proximity Warning System alerts	2.6 %
Separation reasons	**4.1 %**
Lateral separation	3.8 %
TCAS	0.3 %
Unknown	**1.1%**
Unknown	1.1 %
POTENTIALLY COMMON CAUSE	**40.2 %**
Late/no landing clearance	**21.2 %**
Blocked R/T, ATCo busy	2.6 %
Landing runway occupied by aircraft	16.6 %
Landing runway occupied by other	2.0 %
Weather	**19.0 %**
Visibility / Runway Visual Range / cloud base	5.0 %
Wind (gust)	5.5 %
Wind shear	6.9 %
Lightning / showers	1.6 %
Percentage	**100%**

Table 2 Percentages of controller reported reasons for initiation of a go around at Schiphol airport.

Further analysis of the go around (GA) reports has shown that there were 21 reported double (or triple) GA's within 4 minutes, from which 15 are subsequent GA's of aircraft that were approaching the same runway under proper separation conditions. This leaves 6 double or triple GA's on converging runways (all within 2 minutes):

- One coincidentally double GA,
- One double GA caused by severe wind during Mixed mode operation, i.e. departure in between arrivals.
- One triple GA caused by Meteo info down,
- One double GA caused by Tower R/T down,
- One triple GA and one double GA caused by severe Wind.

It was also verified if any of these double or triple GA's had led to a critical incident; it turned out that none of them had done so.

On the basis of these statistical GA data and expert based estimates of relevant exposure frequencies and GA reporting reliability, double GA frequencies have been estimated, they are given in Table 3 and referred to as **Model Assumption M.30a**.

Double GA due to Mixed mode operation	$\hat{\rho}_{\text{Mixed}} = 4.0 \cdot 10^{-4}$
Single GA	$\hat{\rho}_{\text{Single}} = 1.24 \cdot 10^{-3}$
Coincidentally double GA	$\hat{\rho}_{\text{Coinc}} = 0.15 \cdot 10^{-5}$
Double GA due to Tower R/T blocked	$\hat{\rho}_{\text{Tower}} = 1.0 \cdot 10^{-5}$
Double GA due to severe Wind	$\hat{\rho}_{\text{Wind}} = 1.75 \cdot 10^{-5}$
Double GA due to Meteo info down	$\hat{\rho}_{\text{Meteo}} = 1.25 \cdot 10^{-5}$
Double GA due to great Alert	$\hat{\rho}_{\text{Alert}} = 0.5 \cdot 10^{-5}$

Table 3 Estimated GA frequencies.

Due to the use of a Bayesian estimation approach the uncertainty in the estimated frequency values is also known. For all except mixed mode, the 95% uncertainty interval for the frequency values goes a factor 1.5 up and a factor 1.5 down. For mixed mode, this uncertainty interval is a factor 1.5 squared.

2.3 Go around initiation heights

For go around initiation height, use has been made of world wide KLM pilot go around reports over the time period September 1992 to May 1994 (Blom et al., 2001b). This data provides an indication for the reasons of initiating a go around, and altitude and frequency of occurrence. Based on this data, a histogram has been constructed of go around initiation heights. Subsequently, this histogram has been fitted with a weighted sum of a Rayleigh density and a uniform density as depicted in Figure 2. The probability density function of go around initiation height is a density fit of this histogram, which is a weighted sum of Rayleigh density (60%) with mean 300ft and a Uniform density (40%). This is referred to as **Model assumption M.4**.

It is also assumed that for each of the double GA causes in Table 3 only one of the following two densities applies:

- The Rayleigh density for double GA's initiated due to Tower R/T blocked and due to severe Wind.
- The uniform density for all other double GA's.

Since the histogram is based on the world-wide trip reports of one airline, there may be a significant uncertainty level in the

shape of the histogram, and thus in the fitted densities (60% Rayleigh and 40% Uniform).

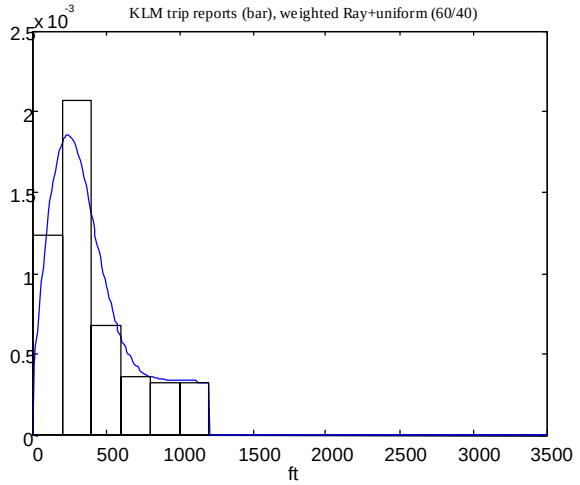

Figure 2 Histogram of KLM pilot GA trip reports and of density fit which is a weighted sum of a Rayleigh density (60%) with mean 300ft and a Uniform density on 0-1200ft (40%).

2.4 Go around climb behaviour

Based on (ICAO-CRM, 1980), probabilistic models for the lateral deviations from nominal missed approach paths are available; this is referred to as **Model assumption M.6a.** For vertical behaviour during go around, ICAO-CRM provides a parabolic vertical path model for the change from descent to climb, and then a model for minimum climb rate requirement only (2.5%). The parabolic vertical path model has been adopted as **Model assumption M.6c**, and the minimal climb rate requirement is used for 1% of the go around climbs to cover non-nominal climbs.

McCartor et al. (1997) provides histograms of simulated FMS-LNAV climb performance during MA's. As a reasonable approximation of these densities, we assumed a Gaussian density with mean value 10 m/s and standard deviation of 2 m/s for the other 99% go arounds. This particular combination of models is referred to as **Model assumption M.5.**

The rate of climb is assumed to continue until the final missed approach altitude has been reached; this is referred to as **Model assumption M.18.** In reality aircraft level off gradually on autopilot, or may overshoot when levelling off without autopilot.

Once the final missed approach altitude has been reached it is assumed that for all aircraft weight categories (heavy, medium and light), the vertical deviations at final MA altitude are assumed to be Gaussian with standard deviation of 10 m. This is referred to as **Model assumption M.6b**. The true standard deviation may be up to a factor 2 larger or smaller, and thus there is a significant uncertainty

2.5 Turn during go around

Although in most cases a turn is made when it is prescribed by the AIP, there is a non-zero miss probability α_{AIP} that a pilot forgets to make a turn during the go around as prescribed in the AIP. Assuming that the pilots are well aware of the AIP published MA path, i.e. **Model assumption M.11**, the expert based estimated values for α_{AIP} vary from 0.05 to 0.22, with 0.10 as best estimate. The last value is referred to as **Model assumption M.29**.

Based on information collected in (Speijker et al., 2000) from experienced (airline) pilots on various aircraft, it was identified that the logical moment at which the pilot starts a turn during a go around is where the pilot completes a well trained sequence of aircraft reconfiguration activities and the aircraft has reached sufficient height. This expert knowledge has resulted into probabilistic models for the reconfiguration of an aircraft during go around, which are referred to as **Model assumption M.20**, and the details of which are given for Boeing 737 and Airbus A320 in Table 4. A similar model has been identified for Boeing 767/300, Boeing 747, Fokker 50, Cessna 172 and Swearingen Metro II.

Task	Starts at	Duration		Ends at
		50%	95%	
1	T1	1 s	3 s	T2
2	T2	6 s	9 s	T3
3	T1 + 1 second	4 s	8 s	T4
4	T1 + 2 seconds	6 s	10 s	T5
5	T4	3 s	10 s	T6
6	T6 & passed 1000 ft	1300 ft	1600 ft	T7
7	T6 & passed 400 ft	600 ft	900 ft	T8
8	Passed altitude of 2000 ft – (10% of climb rate in fpm)	1700 ft	1900 ft	T9

Table 4 Boeing 737 / Airbus A320 go around task breakdown. T1 is the go around initiation moment. The tasks are: 1) Triggering go around flight director mode, 2) Thrust change to go around thrust, 3) Adjusting pitch angle, 4) Raising flaps to climb-out setting, 5) Raising the gear, 6) Engaging the autopilot, 7) Turn. Adjusting lateral navigation, 8) Level off, Adjusting vertical navigation.

In addition, Boeing 747 and 767/300 are assumed to be representative for heavy category aircraft. Boeing 737 and Airbus A320 are assumed to be representative for 50% of medium category aircraft, while Fokker 50 is assumed to be representative for the other 50% of the medium weight aircraft. Swearingen Metro II and Cessna 172 are each assumed to be representative for 50% of the light category aircraft.

2.6 Controller turn instructions

If aircraft on runways 22 and 19R both make a go around then the way of working is that the 19R runway controller issues a preventive right turn instruction to the aircraft on 19R. It is assumed that the controllers of runways 19R and 22 monitor aircraft well on initiating a go around and inform each other immediately of such event. This is referred to as **Model assumption M.10**. It is assumed that the controller of runway 22 does not issue a manoeuvre instruction (**Model assumption M.31**). Subsequently the instruction by the 19R controller should reach the pilots of aircraft on 19R. The chances to accomplish this vary significantly with the double GA causing conditions. Expert estimates for the probability that a 19R controller is not successful in letting the pilot on 19R make a right turn in case of a double go around are provided in Table 5. The expected values are referred to as **Model assumption M.30b.**

A properly received ATCo turn instruction is assumed to be implemented by the pilot immediately upon completion of the

reconfiguration activities. This is referred to as **Model assumption M.12**. It is also assumed that this reception of such instruction from the controller does not lead to any delay in the completion of the reconfiguration tasks (**Model assumption M.13**).

Symbol	Expected	Max	Min
α_{Mixed}	0.05	0.10	0.02
α_{Coinc}	0.15	0.30	0.05
α_{Tower}	0.50	0.99	0.25
α_{Wind}	0.15	0.30	0.05
α_{Alert}	0.05	0.10	0.02
α_{Meteo}	0.05	0.10	0.02

Table 5 Expert estimated values for the probability that the 19R controller is not successful in letting the aircraft on 19R make a right turn in case of a double go around.

In order to validate **M.12**, **M.13** and **M.20** to a reasonable extent, KLM has performed Boeing 737 flight simulator sessions with 21 different flight crews, in which a sudden runway non-availability was simulated. Subsequently, during the rejected landings a pseudo controller suddenly issued a turn instruction. The observed moments of starting a turn agreed quite well with the probabilistic model. It also became clear that during these simulator sessions, sharper turns were realised than assumed in the model.

3. MATHEMATICAL MODELLING

3.1 Integration of mathematical models

For the integration of the mathematical models, the Dynamically Coloured Petri Net (DCPN) approach is used (Everdij et al., 1997; Everdij and Blom, 1999). During DCPN development, use is made of a functional representation of ATM. The functional subsystems and their interrelations are depicted in Figure 3.

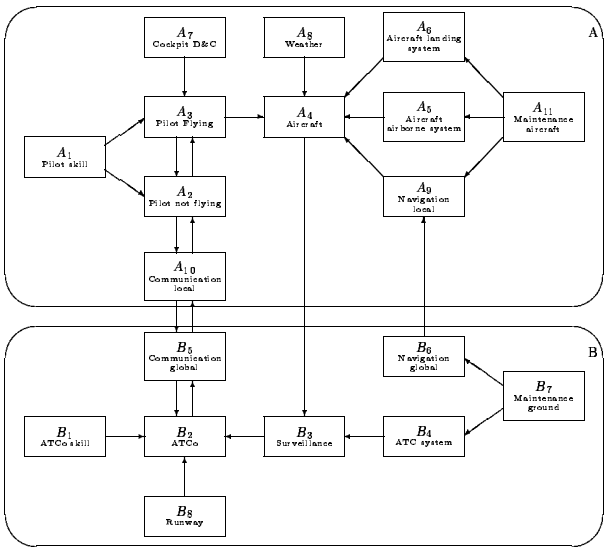

Figure 3 Functional representation of ATM.

For this particular risk assessment application it appeared to be sufficient to develop a Petri net for the aircraft evolution only. One such Petri net is necessary for each aircraft separately. This Petri net is represented by the graph in Figure 4. This graph consists of three kinds of symbols *places* ○, *transitions* □ and *arcs*, which go either from a place to a transition or vice versa. In this Petri net, the places correspond to physical flight segments. The identified flight segments are determined by the following points: Outer Marker (OM), Minimum Radar Vectoring Altitude (MRVA), Touchdown (TD), Go around (GA) and Final MA Altitude (FMAA).

The dynamic status of the Petri net is shown through the appearance of one or more tokens in places and a dynamic colour value connected to each token. In a DCPN, a token colour value may evolve according to a (stochastic) differential equation, the characteristics of which depend on the place of the token. The solution of such differential equation may for example represent the evolution of the aircraft.

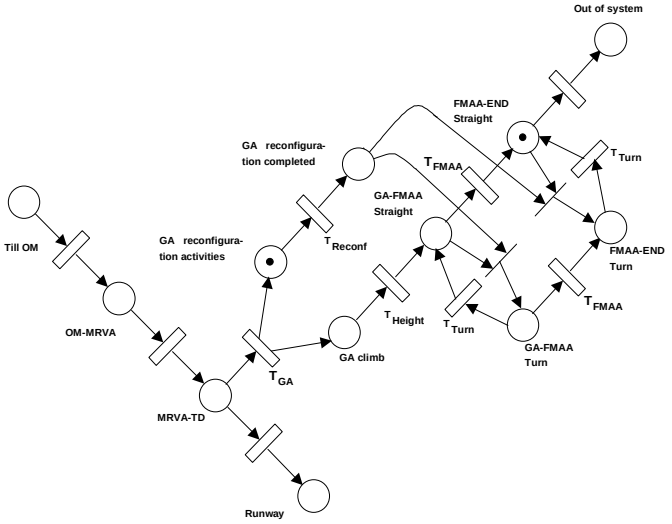

Figure 4 Aircraft evolution Petri net: detailed level. Drawn is a feasible two token situation, one token in place 'GA reconfiguration activities' and one token in place 'FMAA-END Straight'. Then the immediate transition to 'FMAA-END Turn' will fire as soon as the guard function of T_{Reconf} evaluates to true.

The Petri net in Figure 4 has two immediate transitions: 1) To GA-FMAA turn, and 2) To FMAA-END turn. These transitions are executed (fired) as soon as the transition is enabled (i.e. there is a token in each place from which there is an arc). All other transitions are guard transitions, which means that from the moment that the transition is enabled an additional condition has to become true prior to the actual firing of the transition. Table 6 specifies these guard transition delays.

On the basis of such a DCPN specification it is rather straightforward to make a software implementation which allows to run Monte Carlo simulations. In theory, collision risk assessment is then a matter of running Monte Carlo simulations and then counting the events that aircraft shapes are physically overlapping. In practice, this approach finds its limitation in the number of Monte Carlo simulations that can reasonably run within a few hours. And when running a million Monte Carlo runs, the assessed collision frequency is significant up to the level of 1E-5 only. In order to improve on this, stochastic analysis is used to decompose the collision risk in parts each of which can be assessed separately. In order to

take maximal advantage of the particular encounter situation under study and the statistical data available, the development of such a risk decomposition is situation specific. Below, we outline how this is done for the double go around scenario, following (Blom et al., 2001b).

Transition	Guard function evaluates to True if:
To OM-MRVA	Aircraft passes OM abeam
To MRVA-TD	Aircraft passes MRVA
To Out of system	Aircraft travelled 25km beyond threshold
T_{GA}	Aircraft reaches a randomly drawn altitude to start the go around.
T_{Height}	Pilot decides that aircraft has reached sufficient altitude to turn.
T_{Reconf}	Aircraft reconfiguration activities are completed
T_{Turn}	The prescribed or instructed turn is completed
T_{FMAA}	Aircraft reaches final Missed Approach altitude
To runway	Touch Down of aircraft

Table 6 Guard transitions in Figure 4.

3.2 Risk of collision between aircraft

Let $y_t^i := (y^i_{x,t}, y^i_{y,t}, y^i_{z,t})$ and $v_t^i := (v^i_{x,t}, v^i_{y,t}, v^i_{z,t})$ be the 3D location and 3D velocity of aircraft *i*; the subscripts *x* and *y* refer to the axis system in Figure 1, and subscript *z* stands for the height. Let $y_t^{ij} := y_t^i - y_t^j$ be the distance between aircraft *i* approaching runway 19R and aircraft *j* approaching runway 22 at time *t* and let $v_t^{ij} := v_t^i - v_t^j$ be the relative velocity of aircraft *i* on runway 19R and aircraft *j* on runway 22 at time *t*.

Define D^{ij} as the collision area of $\{y_t^{ij}\}$, such that $y_t^{ij} \in D^{ij}$ means that at moment *t* the physical volumes of aircraft *i* and *j* are not separated anymore, i.e. they have collided. For aircraft encounters on final MA altitude, the collision area D^{ij} is a rectangular box, defined as $[-d_x^{ij}, d_x^{ij}] \times [-d_y^{ij}, d_y^{ij}] \times [-d_z^{ij}, d_z^{ij}]$, with $d_r^{ij} \equiv \frac{1}{2} d_r^i + \frac{1}{2} d_r^j$ and where the parameters d_x^i, d_y^i and d_z^i represent *x*, *y* and *z*-direction sizes of aircraft *i* respectively. For aircraft encounters during MA climb, the collision area D^{ij} depends on the inclination angle of the aircraft.

It is possible that the process $\{y_t^{ij}\}$ enters the area D^{ij} several times; each such occurrence is called an incrossing. Each occurrence of the process $\{y_t^{ij}\}$ leaving the area D^{ij} is called an outcrossing. The first incrossing for aircraft pair (*i*,*j*) on runways 19R and 22 is a collision for that pair. Hence, the incrossing rate is an upper bound for collision rate. Under the assumption that the relative speed v_t^{ij} is very rapidly going to zero as long as y_t^{ij} resides in D^{ij}, it is highly improbable that there is more than one incrossing per aircraft pair, and thus the expected number of incrossings is a tight upper bound of the expected number of collisions. By using this approach the tightness of the upper bound can be verified.

Following reference (Bakker and Blom, 1993), the risk of collision *R* between two aircraft is expressed to be equal to a tight upper bound for the expected number of incrossings, between one aircraft *i* and another aircraft *j* in an appropriate time-interval [*0,T*] as follows

$$R = \int_0^T \varphi^{ij}(t)\, dt \tag{1}$$

where $\varphi^{ij}(t)$ is the incrossing rate between aircraft *i* and *j*, which is defined as

$$\varphi^{ij}(t) \equiv \lim_{\Delta \downarrow 0} \frac{P(y_t^{ij} \notin D^{ij},\, y_{t+\Delta}^{ij} \in D^{ij})}{\Delta} \tag{2}$$

In the remainder, time *T* is always chosen large enough such that the probability that the aircraft pair (*i*,*j*) collides outside interval [*0, T*] is negligible small.

3.3 Collision risk per approach

Now define R_Σ as the probability that aircraft *i* makes a GA on 19R and collides with an aircraft making a GA on runway 22. Also define *stopping times* τ^i and τ^{ij} for aircraft *i* and the pair (*i, j*) as

$$\tau^i \equiv \inf \left\{ T, t \,\middle|\, \text{Aircraft } i \text{ initiates a GA at } t \right\}$$

and

$$\tau^{ij} \equiv \max \left\{ \tau^i, \tau^j \right\}.$$

From equation (1) and the definition of τ^{ij} it follows that R_Σ satisfies

$$R_\Sigma = \sum_j \int_{\tau^{ij}}^T \varphi^{ij}(t)\, dt \tag{3}$$

where the summation is over all runway 22 aircraft *j*.

3.4 Aircraft types and double GA causes

The event sequence classification process $\left\{ \kappa_t^{ij} \right\}$ for an aircraft pair *(i,j)* consists of a local (i.e. aircraft) related process and a common related process. Here, this process is defined as $\kappa_t^{ij} \equiv \text{Col} \left\{ \kappa^i,\ \kappa^j, \kappa_t^G \right\}$, where κ^i and κ^j represent the aircraft types considered for aircraft *i* and *j* respectively, and where the process $\left\{ \kappa_t^G \right\}$, with $\kappa_t^G \in K^G$, represents the specific GA condition for both aircraft *i* and *j*. The set K^G represents a set of double GA's due to various reasons, i.e.

$K^G \equiv \{\text{Coinc, Mixed, Tower, Wind, Alert, Meteo}\}$.

Now, we identify the value of $\left\{ \kappa_t^{ij} \right\}$ at moment τ^{ij} as a relevant *event sequence class* $\kappa_{\tau^{ij}}^{ij}$. Hence

$\kappa_{\tau^{ij}}^{ij} \equiv \text{Col} \left\{ \kappa^i,\ \kappa^j, \kappa_{\tau^{ij}}^G \right\}$.

Conditioning on event sequence class $\kappa_{\tau^{ij}}^{ij}$ and rearranging summation and integral yields

$$R_\Sigma = \sum_j \sum_{\kappa \in K} P\left\{ \kappa_{\tau^{ij}}^{ij} = \kappa \right\} \int_{\tau^{ij}}^T \varphi_\kappa^{ij}(t)\, dt \tag{4}$$

where set *K* is defined as $K \equiv K^i \otimes K^j \otimes K^G$ and K^i and K^j are sets of aircraft types for aircraft *i* and aircraft *j*. Moreover,

$\varphi_{\kappa}^{ij}(t)$ is the $\kappa_{\tau^{ij}}^{ij}$ conditional incrossing rate between aircraft *i* and aircraft *j*, with aircraft *i* on one runway and aircraft *j* on the other runway, which is defined as

$$\varphi_{\kappa}^{ij}(t) \equiv \lim_{\Delta \downarrow 0} \frac{P(y_t^{ij} \notin D^{ij},\, y_{t+\Delta}^{ij} \in D^{ij} \,\big|\, \kappa_{\tau^{ij}}^{ij} = \kappa)}{\Delta}$$

3.5 Decomposition over manoeuvre combinations

Through adopting some technical assumptions and a lengthy derivation it is possible to extend the risk decomposition of equation (4) to go around manoeuvre combinations and to identify what the summation over *j* means in terms of Monte Carlo simulations. The resulting set of equations is (Blom et al., 2001b):

$$R_{\Sigma} = \sum_{\kappa^G \in K^G} R_{\kappa^G} \tag{5}$$

$$R_{\kappa^G} = \hat{\rho}_{\kappa^G} \sum_{w_{19R} \in W_{19R}} \sum_{w_{22} \in W_{22}} p_{\kappa^G}(w_{19R}) \cdot p_{\kappa^G}(w_{22}) \cdot \mu_{\kappa^G}(w_{19R}, w_{22}) \tag{6}$$

with W_z a set of two possible MA paths for runway *z*.

$$\begin{aligned} p_{\kappa^G}(w_{19R}) &= \alpha_{\kappa^G} && \text{if} \quad w_{19R} = \text{straight \& 2000 ft} \\ &= (1-\alpha_{\kappa^G}) && \text{else} \\ p_{\kappa^G}(w_{22}) &= \alpha_{\text{AIP}} && \text{if} \quad w_{22} = \text{straight \& 2000 ft} \\ &= (1-\alpha_{\text{AIP}}) && \text{else} \end{aligned}$$

And for $w \in W_{19R} \times W_{22}$

$$\begin{aligned} \mu_{\kappa^G}(w) = 2 \cdot \sum_{\kappa^a,\, \kappa^b} & P\left\{\left(\kappa_{\tau^{il}}^{i}, \kappa_{\tau^{il}}^{l}\right) = \left(\kappa^a, \kappa^b\right)\right\} \\ & \cdot I^{il}\left(\left(\kappa^a, \kappa^b, \kappa^G\right), w\right) \end{aligned} \tag{7}$$

$$I^{il}(\kappa, w) \equiv \int_{\tau^{il}}^{T} \varphi_{\kappa}^{il}(t, w)\, dt$$

with *l* such that (τ^l - τ^i) has a uniform distribution on [-180s, 60s].

3.6 Decomposition of incrossing rate

Following (Bakker and Blom, 1993), the conditional incrossing rate satisfies

$$\begin{aligned} \varphi_{\kappa}^{il}(t, w) = \sum_{r=x,y,z} \int_{\underline{D}_r} \Bigg\{ & \int_0^{\infty} v_r^{il}\; p_{y_t^{il} v_{r,t}^{il} | \kappa_{\tau^{il}}^{il}}\left(\underline{y}_r^{il}, -d_r^{il}, v_r^{il} \,|\, \kappa, w\right) dv_r^{il} \\ & + \int_{-\infty}^{0} -v_r^{il}\; p_{y_t^{il} v_{r,t}^{il} | \kappa_{\tau^{il}}^{il}}\left(\underline{y}_r^{il}, d_r^{il}, v_r^{il} \,|\, \kappa, w\right) dv_r^{ij} \Bigg\}\, d\underline{y}_r^{il} \end{aligned} \tag{8}$$

where $p_{y_t^{il} v_{r,t}^{il} | \kappa_{\tau^{il}}^{il}}(\kappa, w)$ is the conditional probability density function for the aircraft relative position and velocity, $\underline{D}_r$ is equal to collision area D^{il} but without the *r*-th component, and $\underline{y}_r^{il}$ for *r* = *x,y,z* is equal to the aircraft relative position without the *r*-th component.

Next, for an aircraft *i* and an aircraft *l*, *stopping times* τ_r^{il} for *r*=*x,y,z* are defined as follows

$$\tau_r^{il} \equiv \inf\left\{ t \geq \tau^{il} \,;\, \left| y_{r,t}^{il} \right| \leq d_r^{il} \right\}$$

Together with (7) and (8) this implies

$$\begin{aligned} & I^{il}(\kappa, w) \\ & = \sum_{r=x,y,z} \int_{\tau_r^{il}}^{T} \int_{\underline{D}_r} \Bigg\{ \int_0^{\infty} v_r^{il}\; p_{y_t^{il} v_{r,t}^{il} | \kappa_{\tau^{il}}^{il}}\left(\underline{y}_r^{il}, -d_r^{il}, v_r^{il} \,|\, \kappa, w\right) dv_r^{il} \\ & + \int_{-\infty}^{0} -v_r^{il}\; p_{y_t^{il} v_{r,t}^{il} | \kappa_{\tau^{il}}^{il}}\left(\underline{y}_r^{il}, d_r^{il}, v_r^{il} \,|\, \kappa, w\right) dv_r^{il} \Bigg\}\, d\underline{y}_r^{il}\, dt \end{aligned} \tag{9}$$

3.7 Numerical evaluation of equations

To assess risk numerically, first equation (9) is evaluated. For each relevant (κ, *w*) the following steps are performed:

- Monte Carlo simulation of double GA's on runways 19R×22.
- This yields histograms of simulated statistical information for the relative aircraft positions and speeds, to which sums of Gaussian densities are fitted.
- Eq. (9) is solved through analytical integration over dv_r^{il} and numerical integration over $d\underline{y}_r^{il}$ and *dt* respectively.
- Finally, the numerical results for $I^{il}(\kappa, w)$ are substituted into equation (7) and this into (5) and (6).

These steps are done with support of the TOPAZ toolset.

4. RISK ASSESSMENT OF OPERATIONAL SCENARIOS

In this section, the risk assessment model is used to evaluate several SCIA operational scenarios for runway 19R×22. First, a series of operational scenarios is defined. Subsequently the risk assessment is performed in a sequence of steps. Finally, a comparison is made against established risk criteria.

4.1 Operational scenarios

The operational scenario variables identified for evaluation are:

- AIP published MA path for runway 19R: *Straight MA path* versus *Right Turn MA path*.
- Mixed mode operations: *Allowed* versus *Not allowed*.
- Instructions by runway controller: *None* versus *Turn on 19R* versus *Extra climb on 19R*.

In total this yields 12 combinations, of which the ones in Table 7 are selected for risk assessment.

Operational scenario	19R MA in AIP	ATCo instruction	Mixed mode allowed
0	Straight MA on 19R	None	Yes
1	Straight MA on 19R	Turn on 19R	Yes
2	Straight MA on 19R	None	No
3	Straight MA on 19R	Turn on 19R	No
4	Straight MA on 19R	Extra climb on 19R	No
5	Turn MA on 19R	None	Yes
6	Turn MA on 19R	None	No

Table 7 Operational scenarios for risk assessment.

For each of these Operational scenarios in Table 7, the set of equations (5-9) has to be evaluated in a numerical sense. This is organised in two steps:

- Assess conditional collision risks $\mu_{\kappa^G}(w)$ using eqs. (7,9)
- Assess collision risk R_{κ^G} and R_Σ using eqs. (5,6)

During subsequent third and fourth steps, bias and uncertainty in the risk values is assessed following (Everdij and Blom, 2001), and the bias and uncertainty corrected risk levels are compared against established risk criteria. The results of these four steps are given in the following four subsections.

4.2 Model based conditional collision risk

To assess the conditional collision risks $\mu_{\kappa^G}(w)$ for each of the operational scenarios in Table 7, eqs. (7) and (9) have to be evaluated in a numerical sense. At the level of $I^{il}(\kappa, w)$ this leads to 4200 (=7×5×5×6×4) combinations, and at the level of $\mu_{\kappa^G}(w)$ this leads to 168 (=7×6×4) combinations. Fortunately, for many of these combinations it can be verified that they are equivalent qua risk. For this particular application the effective number of combinations that have to be evaluated at the $I^{il}(\kappa, w)$ and $\mu_{\kappa^G}(w)$ levels amounts 120 (= 4×3×2×5) and 12 respectively. The risk values $\mu_{\kappa^G}(w)$ assessed for the latter 12 combinations are given in Table 8.

w_{19R}	w_{22}	$\kappa^G \in$ {Tower, Wind} Rayleigh PDF	Other κ^G Uniform PDF
Straight	Straight	2.9 E-3	2.9 E-3
Straight	Left turn	3.7 E-8	2.4 E-8
Right turn	Straight	4.1 E-8	2.5 E-8
Right turn	Left turn	2.6 E-8	1.8 E-8
Extra climb	Straight	1.2 E-5	1.1 E-5
Extra climb	Left turn	< 3.7 E-8	< 2.4 E-8

Table 8 Conditional collision risk values $\mu_{\kappa^G}(w)$.

As expected, all risk values of the Rayleigh PDF GA initiation height are higher than those for the Uniform PDF GA initiation height; the only exception is formed by the risk values for both aircraft making a straight GA. Also as expected is that the conditional collision risk values are worst when both aircraft make a straight GA. However, these risk values are almost five orders of magnitude worse than the risk values in case at least one of the aircraft makes a turn. The implication is that as long as there is a small chance that both aircraft make straight GA's then the conditional risk values at the top of Table 8 determine the total risk, and this is neutral regarding the precise shape of the GA initiation height PDF. This corresponds with the key finding of the phase 1 study (Blom et al., 2001a). Another observation that can be made is that for the runway combination considered a turn appears to be more effective than an extra climb of 500 ft.

4.3 Model based collision risk

The next step in the assessment of collision risk is to evaluate equation (6) per scenario, using the conditional collision risk values from Table 8 and the $\hat{\rho}_{\kappa^G}$, α_{κ^G} and α_{AIP} values as these have been estimated in section 2, taking into account the following specific adaptation sequence:

- No Mixed Mode allowed means: $\hat{\rho}_{Mixed} = 0$
- Right turn MA on 19R in AIP means: replace α_{κ^G} by α_{AIP}
- No ATCo instruction means: replace α_{κ^G} by 1

The resulting collision risk values are presented in Table 9. This shows that the model based total risks vary up to a factor 100 with the scenario, with scenario 0 having highest risk and scenarios 3, 4 and 6 having lowest risk. Before drawing further conclusions it is better to assess bias and uncertainty in these risk values first.

Scenario	0	1	2	3	4	5	6
R_{Mixed}	1.2E-07	5.8E-09	0	0	0	1.2E-08	0
R_{Coinc}	4.5E-10	6.7E-11	4.5E-10	6.7E-11	6.9E-11	4.5E-11	4.5E-11
R_{Tower}	2.9E-09	1.5E-09	2.9E-09	1.5E-09	1.5E-09	2.9E-10	2.9E-10
R_{Wind}	5.1E-09	7.6E-10	5.1E-09	7.6E-10	7.8E-10	5.1E-10	5.1E-10
R_{Alert}	1.5E-09	7.3E-11	1.5E-09	7.3E-11	7.8E-11	1.5E-10	1.5E-10
R_{Meteo}	3.6E-09	1.8E-10	3.6E-09	1.8E-10	1.9E-10	3.6E-10	3.6E-10
R_Σ	**1.3E-07**	**8.3E-09**	**1.3E-08**	**2.5E-09**	**2.6E-09**	**1.3E-08**	**1.4E-09**

Table 9 Model based collision risks for SCIA on 19R×22.

4.4 Bias and uncertainty assessment

The risk values in Table 9 apply to the mathematical model of the operational scenarios. Since such a mathematical model differs from reality one should expect that the model based risk differs from the true risk also. The question then is to assess this difference in terms of bias and uncertainty relative to the model based risk. Recently, Everdij and Blom (2001) have developed a methodology to conservatively assess the bias and the 95% uncertainty band due to these differences. To apply this methodology to the SCIA scenarios of Table 9, we first give the equations of the total expected risk R_Σ^* :

$$R_\Sigma^* = B \cdot \exp\left\{\tfrac{1}{8} C\right\} \cdot R_\Sigma \qquad (10)$$

with bias factor B and 95% uncertainty band (up and down) factor $\exp\sqrt{C}$ satisfying:

$$B = f_{\text{C}}^{\,(n_{\text{CO}} - n_{\text{CP}})} \cdot f_{\text{S}}^{\,(n_{\text{SO}} - n_{\text{SP}})} \cdot f_{\text{M}}^{\,(n_{\text{MO}} - n_{\text{MP}})} \cdot f_{\text{Sm}}^{\,(n_{\text{SmO}} - n_{\text{SmP}})} \cdot f_{\text{N}}^{\,(n_{\text{NO}} - n_{\text{NP}})} \qquad (11)$$

$$C = n_{\text{CU}} \cdot (\ln f_{\text{C}})^2 + n_{\text{SU}} \cdot (\ln f_{\text{S}})^2 + n_{\text{MU}} \cdot (\ln f_{\text{M}})^2 + n_{\text{SmU}} \cdot (\ln f_{\text{Sm}})^2 + n_{\text{NU}} \cdot (\ln f_{\text{N}})^2 \qquad (12)$$

where $n_{\text{XY}} \equiv$ total number of XY valued model assumptions, with X ∈ {Considerable (C), Significant (S), Minor (M), Small (Sm), Negligible (N)}, and with Y ∈ {Pessimistic (P), Uncertain (U), Optimistic (O)}, and with factors

$$\begin{aligned} f_{\text{C}} &= f_M^{\,4} &&\approx 5.06 \\ f_{\text{S}} &= f_M^{\,2} &&= 2.25 \\ f_{\text{M}} & &&= 1.5 \\ f_{\text{Sm}} &= \text{sqrt}(f_{\text{M}}) &&\approx 1.2 \\ f_{\text{N}} &= \text{sqrt}(f_{\text{Sm}}) &&\approx 1.1 \end{aligned}$$

	0	1	2	3	4	5	6
SP	M.31	M.31	M.31	M.31	M.31	M.31	M.31
MP	-	-	-	-	-	-	-
SmP	-	-	-	-	-	-	-
NP	7×	7×	7×	7×	7×	7×	7×
CU	-	-	-	-	-	M.29	M.29
SU	M.29 M.30a	M.29 M.30a M.30b	M.29	M.29 M.30b	M.29 M.30b	M.30a	-
MU	M.6b	M.6b	M.6b M.30a	M.6b M.30a	M.6b M.30a	M.6b	M.6b M.30a
SmU	2×	3×	2×	3×	3×	2×	2×
NU	20×	20×	20×	20×	20×	20×	20×
SO	-	-	-	-	-	-	-
MO	-	-	-	-	-	-	-
SmO	-	-	-	-	-	-	-
NO	5×	5×	5×	5×	5×	5×	5×

*Table 10 Overview of main results of expected effects of assumptions on the collision risk for the various scenarios. The model assumptions are introduced in section 2. Model assumption **M.15** (No TCAS) is not evaluated.*

Here, pessimistic expected direction means that the modelled risk increases due to the assumption (i.e. the expected risk will be smaller than the model based risk). Optimistic expected direction means that the modelled risk reduces due to the assumption (i.e. the expected risk will be larger). Uncertainty expected direction means that it is expected that the influence on the modelled risk results is uncertain.

In this approach, positive and negative bias factors may (partly) compensate each other while uncertainty band factors accumulate in a non-linear way. This approach requires safety conservative assessment of model assumptions against reality. Due to such safety conservatism the chance that risk falls above and below the assessed uncertainty band is 2.5% or less and 2.5% or more respectively.

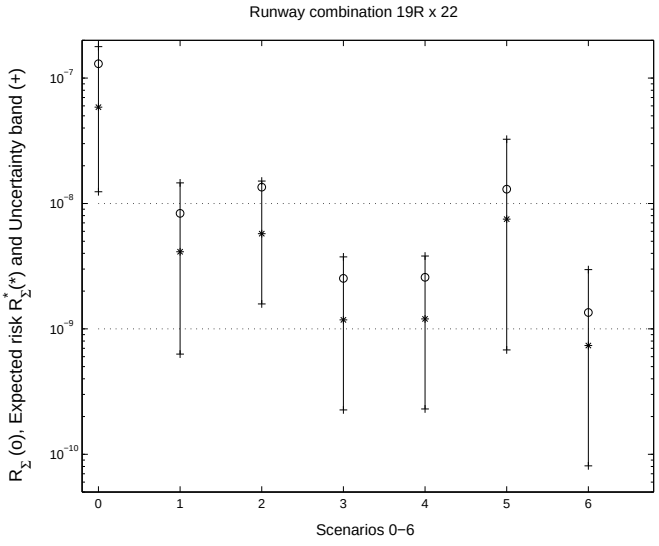

Figure 5 Model based risk R_Σ (o), expected risk R^*_Σ (*) and uncertainty band (++), assuming No TCAS.

To assess the impact of all assumptions on collision risk and to determine uncertainty bands, all modelling assumptions except **M.15** (i.e. no TCAS) are assessed in a particular sequence to take into account dependencies (Everdij and Blom, 2001). In case of lack of knowledge, a safety conservative approach has been taken. For parameter value assumptions the contribution to the uncertainty is assessed with support of model based parameter sensitivity analysis. The results of this assessment are presented in Table 10.

By counting the n_{XY}'s in Table 10 and substituting this in eqs. (10-12) we get the results in Figure 5 and in the last row of Table 11. To complete Table 11, we use $R^*_{\kappa^G} = R_{\kappa^G} \cdot \frac{R^*_\Sigma}{R_\Sigma}$.

Scenario	0	1	2	3	4	5	6
R^* Mixed	5.3E-08	2.9E-09	0	0	0	6.7E-09	0
R^* Coinc	2.0E-10	3.3E-11	1.9E-10	3.1E-11	3.2E-11	2.6E-11	2.4E-11
R^* Tower	1.3E-09	7.2E-10	1.2E-09	6.7E-10	6.8E-10	1.7E-10	1.6E-10
R^* Wind	2.3E-09	3.8E-10	2.2E-09	3.5E-10	3.6E-10	2.9E-10	2.8E-10
R^* Alert	6.6E-10	3.6E-11	6.2E-10	3.4E-11	3.6E-11	8.4E-11	7.9E-11
R^* Meteo	1.6E-09	9.0E-11	1.5E-09	8.4E-11	9.0E-11	2.1E-10	2.0E-10
R^*_Σ	**5.9E-08**	**4.1E-09**	**5.7E-09**	**1.2E-09**	**1.2E-09**	**7.5E-09**	**7.4E-10**

Table 11 Expected collision risk R^*_Σ for the scenarios, assuming No TCAS.

4.5 Comparison against risk criteria

For the SCIA operation considered, a generally accepted safety requirement does not exist. Nevertheless, relevant comparisons can be made: 1) a comparison with the maximal JAR allowable 1E-9 of catastrophic risk per airborne system failure per flying hour (JAR 25.1309), and 2) a comparison regarding an adequate use of SCIA to reduce the flight arrival delay, and thus also the collision risk exposure due to reduced flying time (e.g. in the stack).

JAR based criterion

If we assume that the average duration of a flight is two hours, then the maximal JAR allowable catastrophic risk per airborne system failure per flight is 2E-9. If we would adopt this same criterion for allowing catastrophic risk per external cause then most of the individual terms in Table 11 appear to satisfy this criterion. The exceptions are the Mixed mode terms in scenarios 0, 1 and 5, and the Wind terms in scenarios 0 and 2. It should be noticed that the effect of TCAS is not taken into account.

ICAO based criterion

To gain further insight we express the expected extra risk in terms of a number of minutes extra flying time that would lead to a similar risk of collision with another aircraft. The rationale behind this is that the reason for conducting SCIA operations is to increase capacity in order to reduce delay (= extra flying time) in the order of minutes per arrival. This reduction in flying time itself implies a reduction in risk of collision with another aircraft (e.g. in the stack). To gain insight in this effect we assume that the exposure of collision with another aircraft corresponds with the TLS adopted by ICAO for fatal accidents per en-route flight hour. Per direction (vertical, lateral, longitudinal) the TLS is $5 \cdot 10^{-9}$ fatal accidents per flight hour (ICAO, 1998), thus for three directions this is $1.5 \cdot 10^{-8}$ fatal accidents per flighthour. Expressing the expected collision risk values of Table 11 in

terms of extra flying minutes with similar risk exposure this yields:

Scenario	0	1	2	3	4	5	6
Extra flying time	236 min.	17 min.	23 min.	5 min.	5 min.	30 min.	3 min.

Table 12 Extra flying time with similar risk exposure.

This shows, if SCIA operation also reduces the flying time per arrival with 5 minutes, then under operational scenarios 3, 4 and 6, the SCIA operation does not increase the total risk per arrival. Practically this means that the risk levels assessed for double GA's during SCIA operation on runways 19R×22 according to scenarios 3, 4 and 6 do not compromise safety; i.e. ATC instructed or AIP prescribed manoeuvre on 19R.

Mitigating measures

Although a series of operational scenarios have been assessed, there are several mitigating measure options which have not been considered in this study, e.g.

- Systematic exploitation of the contribution by TCAS.
- Mitigating measures such that the occurrence of key hazards reduces significantly, i.e. *Tower down*, *severe Wind* and *Meteo down* in particular.
- Training of situation dependent handling by tower air traffic controllers.
- Increase training of pilots for non-straight GA's.

This means that the assessed risk values for conducting SCIA on 19R×22 can be further decreased if so desired.

5. CONCLUSIONS

In this paper a risk assessment has been performed regarding simultaneous instrument approaches on converging runway combination 19R×22 at Schiphol. This is a follow-up of an earlier study in which it has been shown that the lowering of the Decision Height for runway 22 is risk neutral in the model, however the uncertainty in the accident risk levels was larger than what is needed to make a useful comparison against established risk criteria. In line with the accident risk assessment methodology of (Blom et al., 1998), the following activities have been performed in an iterative way:

1. Identify the specific go around scenarios to be assessed, and gather information about nominal and non-nominal behaviour of simultaneous go around by making use of information regarding pilot and ATCo interviews, statistical analysis of various data bases and go around flight simulations conducted by experienced pilots. The results of these activities are given in section 2.
2. Develop a stochastic dynamical model of the operation, including a systematic specification of the additional assumptions adopted. The results of these activities are given in section 3.
3. Perform Monte Carlo simulations and mathematical analysis techniques to assess the model based accident risk for the go around scenarios identified. The results of these activities are given in subsections 4.1-4.3.
4. Perform an assessment of the model assumptions and the impact each of these assumptions has on the accident risks for each go around scenario. The results are given in subsection 4.4.
5. Compare the risk results obtained for SCIA operations on runways 19R×22 to JAR and ICAO established fatal accident risk criteria. This has been done in subsection 4.5.

5.1 Conclusions regarding SCIA on 19R×22

Regarding SCIA on 19R×22 the main findings of the study are:

- The highest risk levels occur when simultaneous converging runway operations would be conducted during mixed mode operations. Mixed mode operations induce significantly higher double GA rates during simultaneous operations on converging runways and therefore the extra risk is significantly higher (factor between 3 to 10) than under non mixed mode operations.
- The expected extra risk values for landing on runway combinations 19R×22 using converging runway operations, and excluding mixed mode operations, lies between 5.7E-9 and 7.4E-10, if TCAS is not taken into account. In both operational scenarios the controller would be doing nothing.
- The identified uncertainty band around the expected risk values extends from about a factor 6 up in risk to a factor 10 or more down in risk. These areas aim to cover 95% of all possibilities for the risk in a conservative way. As such, 2.5% or less may be above the upper bound of the uncertainty band, and 2.5% or more may be below the lower bound of the uncertainty band.
- For some model assumptions, insufficient knowledge forced us to skipp the TCAS assessment and to use an assessment of the impact on the risk which may be conservative. Further investigations of the impact of these assumptions is recommended, with TCAS and pilot/controller responses as the main ones.
- The largest contribution to risk is coming from common causes (even if Mixed mode operations are not allowed). Under some of the important common causes the effectiveness of the controller is significantly lower than the nominal effectiveness is.
- The evaluation of the model assumptions has shown that there are possibilities to improve the instantiated model on the basis of available knowledge. Such improvements would simplify the evaluation of model assumptions; however, the impact on the expected risk is minor only. Areas for such improvements are: Wind model, GA climb and level-off model, Aircraft airspeed model and Aircraft turning model.

Under operational scenarios of an ATC instructed or AIP prescribed manoeuvre on 19R and an AIP prescribed manoeuvre on 22, the level of catastrophic risk due to double missed approaches under SCIA on runways 19R and 22 appeared to be lower than the ICAO (1998) allowed risk of mid-air collision during five minutes en-route flying. Practically this risk level is comparable to the reduction in risk exposure to other aircraft e.g. due to leaving aircraft 5 minutes shorter in stack when conducting SCIA operations on 19R×22. In view of such marginal net differences in risk level, one may conclude that SCIA operation on 19R×22 under these operational scenarios does not compromise safety.

5.2 General conclusions regarding SCIA

The SCIA risk modelling study has revealed a number of issues which have not been addressed in previous studies:

- Common cause double GA's appear far more frequent than coincidental double GA's.
- Some of these common causes also reduce the performance of ATC in a negative way.
- It has been shown that it is possible to conduct SCIA operations at risk levels that are in agreement with risk criteria established by JAR and ICAO.
- The placing of the MAPt may have remarkably little impact on the safety of the SCIA operation.
- There are safety mitigating measures which potentially contribute to the further development of SCIA operations.

For the specific Schiphol example it has been shown that SCIA does not compromise safety; neither in relative nor in absolute terms under conditions that fall outside the current FAA criteria for SCIA operations. For airports with frequent low ceilings it would be valuable to relax these criteria through the adoption of the accident risk assessment methodology discussed in this paper. For an optimal reduction of SCIA criteria a dedicated collection of site specific statistical data on missed approaches and their reasons would be of great value. Since the FAA prescribes a systematic reporting by ATC of simultaneous go around events while conducting SCIA (FAA, 1993) one may expect that such valuable information is available. By using this in combination with a systematic accident risk assessment modelling approach, one might reasonably expect that the TERPS+3 criteria can be relaxed significantly, and in particular on a site specific basis.

6. REFERENCES

AIP, Aeronautical Information Publication, The Netherlands, 2000.

Bakker, G.J. and H.A.P. Blom, Air Traffic Collision risk modelling, Proc. 32nd IEEE Conf. on Decision and Control, 1993, pp. 1464-1469.

Blom, H.A.P., G.J. Bakker, P.J.G. Blanker, J. Daams, M.H.C. Everdij and M.B. Klompstra, Accident risk assessment for advanced ATM, Proc. 2nd USA/Europe ATM R&D Seminar, FAA/Eurocontrol, December 1998, http://atm-seminar-98.eurocontrol.fr

Blom, H.A.P., G.J. Bakker, M.B. Klompstra and L.J.P. Speijker, Risk Analysis of Simultaneous Missed Approaches on Runways 19R and 22, WP2: Modelling and evaluation of collision risk, NLR Report CR-2000-697, February 2001a.

Blom, H.A.P., M.B. Klompstra and G.J. Bakker, Accident risk due to missed approaches on converging runways 19R×22 at Schiphol airport, Part 1: Accident risk assessment, 2001b.

Blom, H.A.P., G.J. Bakker and M.B. Klompstra, Accident risk due to missed approaches on converging runways 19R×22 at Schiphol airport, Part 2: Appendices, 2001c.

Everdij, M.H.C., Blom, H.A.P., Klompstra, M.B., Dynamically coloured Petri Nets for Air Traffic Management safety purposes, 8th IFAC symposium on Transportation Systems, June 16-18, 1997, Chania Greece, NLR Report TP 97493 L, 1997.

Everdij, M.H.C., Blom, H.A.P., Piecewise Deterministic Markov Processes represented by Dynamically Coloured Petri Nets, NLR report TP-2000-428, December 1999.

Everdij, M.H.C., and H.A.P. Blom, Designing EATMS inherently safe, Bias and uncertainty in accident risk assessment, TOSCAII, WP4 phase 2 for Eurocontrol, Draft report, August 2001.

FAA, Simultaneous Converging Instrument Approaches (SCIA), FAA Order 7110.98A, June 23rd 1993.

FAA, Simultaneous Converging ILS Approaches Aided by FMS LNAV Missed Approach, FAA Order 8260.40.C7, December 31st 1998.

ICAO-CRM, Manual on the use of the Collision Risk Model (CRM) for ILS operations, 1st edition, ICAO-Doc-AN/9274, 1980.

ICAO, Simultaneous Operations on parallel or near parallel Instrument Runways (SOIR), ICAO Circular 207-AN/126, Montreal, Canada, 1988.

ICAO, Procedures for Air Navigation Services – Aircraft Operations (PANS-OPS), Volume I: Flight procedures; Volume II: Construction of visual and instrument flight procedures, ICAO Doc 8168-OPS/611, 1996.

ICAO, Annex 11 – Air Traffic Services, 12th edition, incorporating amendments 1-38, Green pages, attachment B, paragraph 3.2.1, July 1998.

JAR 25.1309, Joint Aviation Requirements JAR-25, Large Aeroplanes, Change 14, 27 May 1994 & Amendment 25/96/1 of 9 April 1996, including AMJ 25-1309: System design and analysis Advisory Material Joint, Change 14, 1994.

McCartor, G.R., F. Hasman, A. Jones, J. Yates, S. Ladecky, Independent Converging FMS/LNAV Missed Approach Evaluation, FAA report DOT-FAA-AFS-450-74, June 1997.

Newman, L.C., W.J. Swedish, T.N. Shimi, Requirements for instrument approaches to converging runways, Report numbers MTR-81W230 and FAA-EM-82-4, MITRE, McLean, Virginia, September 1981.

Smith, A.P., A.D. Mundra, D.R. Barker, G.A. Dorfman, The Dependent Converging Instrument Approach procedure: an analysis of its safety and applicability, Final report DOT/FAA/RD-93-006, MITRE, November 1992.

Speijker, L.J.P., A.K. Karwal, G.B. van Baren, H.A.P. Blom, E.A.C. Kruijsen, H.W Veerbeek and J.H. Vermeij, Risk Analysis of Simultaneous Missed Approaches on Runways 19R and 22, WP1: Missed approach model and safety criteria, NLR report CR-2000-645, December 2000.

Weiss, W.E., Proposed single criterion for IFR approaches to converging runways, Report numbers MTR-86W17 and FAA-DL5-86-2, MITRE, McLean, Virginia, July 1986.

ACRONYMS

AIP	Aeronautical Information Publication
ATC	Air Traffic Control
ATCo	Air Traffic Controller
ATM	Air Traffic Management
DCIA	Dependent Converging Instrument Approaches
DCPN	Dynamically Coloured Petri Net
DH	Decision Height
FMAA	Final MA Altitude
FMS	Flight Management System
GA	Go around
ICAO	International Civil Aviation Organisation
ILS	Instrument Landing System
JAR	Joint Aviation Requirements
LNAV	Lateral Navigation
MA	Missed Approach
MAPt	Missed Approach Point
MRVA	Minimum Radar Vectoring Altitude
OM	Outer Marker
PDF	Probability Density Function
R/T	Radio/Telephony
SCIA	Simultaneous Converging Instrument Approaches
TCAS	Traffic Collision Avoidance System
TD	Touchdown
TERPS	Terminal Instrument Approaches
TLS	Target Level of Safety
TOPAZ	Traffic Organization and Perturbation AnalyZer

BIOGRAPHIES

Henk A.P. Blom; National Aerospace Laboratory NLR, Amsterdam, The Netherlands. Henk Blom received a Masters from Twente University (1980) and a Ph D from Delft University of Technology (1990), on the thesis "Bayesian estimation for decision-directed stochastic control". He has more than 20 years research experience in the development of stochastic analysis theory and application in ATM. He is the father of the, in target tracking literature well known, Interacting Multiple Model (IMM) algorithm, of Eurocontrol's Multi-Target-Multi-Sensor Tracking system ARTAS, and of TOPAZ (Traffic Organization and Perturbation AnalyZer). At NLR he is leader of the ATM Modelling research group. His main research interests are in data fusion and probabilistic conflict prediction, and in the development of formal methods towards accident risk assessment of advanced operations in ATM which takes into account the responsibilities and roles of pilots, the air traffic controllers, and their organizations.

Margriet B. Klompstra; National Aerospace Laboratory NLR, Amsterdam, The Netherlands. Margriet Klompstra graduated from Groningen University in Mathematics in 1986 and obtained a Ph D in 1992 from Delft University of Technology. She joined the NLR in 1992, as a member of the ATM modelling group, key areas of research have been risk-sensitive control, application of stochastic dynamic models within ATM, development and application of the accident risk assessment methodology TOPAZ (Traffic Organization and Perturbation AnalyZer).

Bert or Gijsbert J. Bakker; National Aerospace Laboratory NLR, Amsterdam, The Netherlands. Bert Bakker received his Masters in Applied Mathematics from the Twente University in 1989. He joined the NLR in 1992, as a member of the ATM modelling group, to develop stochastic dynamic models as basis for architectural insight, probabilistic safety evaluation of ATM enhancements and practically useful algorithms in advanced ATM. The results have found application (amongst others) in the development of the ATM safety evaluation tool TOPAZ (Traffic Organization and Perturbation AnalyZer). His key contributions are in the theoretical research of collision risk modelling, and on the development and implementation of the ATM safety evaluation tool TOPAZ.